Dynamic simulation of a geothermal reservoir

Case study of the Dinantian carbonates encountered in the Californië geothermal wells, Limburg, NL

Dominique Reith[1], Raymond Godderij[1], Bastiaan Jaarsma[1], Giovanni Bertotti[2], Leonora Heijnen[1]

[1] EBN B.V., Daalsesingel 1, Utrecht, NL

[2] Delft University of Technology, Stevinweg 1, Delft, NL

Dominique.reith@ebn.nl

Keywords: Carbonate reservoir, karst, reservoir quality, exploration, fracture driven permeability

ABSTRACT

In the context of the energy transition, rapid development of the geothermal sector in the Netherlands has to take place. The first steps have been taken by establishing the Green Deal UDG (Ultra Deep Geothermal) between multiple industrial consortia, which agree to share knowledge on the research and use of ultra-deep geothermal energy. The Dinantian carbonates are of interest for the deep geothermal wells, because of their high geothermal potential. This paper provides a case study of the Californië geothermal doublets in Limburg (NL), which are currently the only geothermal wells in the Netherlands producing from the Dinantian carbonates. However, the static and dynamic model prove that the Devonian Bosscheveld formation and Condroz group are also part of the reservoir interval. Due to the tight matrix of the reservoir rocks, the permeability is believed to be fracture- and karst-(meteoric and hydrothermal) driven. This paper describes the static and dynamic models that are created to confirm the current production data (history match) and to explore the development of the geothermal potential of the reservoir in space and time. The static and dynamic reservoir models are based on a limited number of well logs and two 2D seismic lines, which forms a major challenge in this project. A framework of assumptions has been defined to construct a static model and a scenario-based approach has been applied to construct a best-case scenario that matches the production data. A key element in the static reservoir model is the Tegelen fault zone. To estimate the impact of the Tegelen fault zone on the permeability distribution in the reservoir, a fieldwork in an analogue carbonate quarry has been executed. The results are applied in the static model. The dynamic results in this study show that the permeability configuration in the reservoir intervals applied in the best-case scenario results in bottom hole pressure (BHP), flow rate and temperature values that are of the correct order of magnitude and within an acceptable error margin of the production data. Two sensitivity studies have been simulated to determine the range of parameters that may cause an inaccuracy in the results. Additional data acquisition is strongly recommended to validate and optimize the static model, which would result in a dynamic model with an improved history match and a larger predictive power for future production and reservoir management.

1. INTRODUCTION

1.1 Energy transition in the Netherlands

The energy transition in the Netherlands has been set into motion in September 2013, when forty-seven organizations signed the 'Agreement on Energy for Sustainable growth', which stated the necessity of increasing the contribution of renewable energy to the energy mix (Ministry of Economic Affairs and Climate Policy, 2013). The establishment of the Paris Agreement in December 2015 and the publication of the Energy Agenda in March 2017 by the Dutch government further specified the necessary increase of renewable energy by formulating the long-term goal of reducing the CO_2 emission in the Netherlands to practically zero in 2050 (Ministry of Economic Affairs and Climate Policy, 2017). Multiple measures have been formulated to achieve this goal, including the development of geothermal energy as an alternative heat source.

The geothermal environment in the Netherlands is currently quickly evolving. The Green Deal UDG (Ultra Deep Geothermal) has been signed in June 2017 by the Dutch government and multiple industrial consortia. The consortia agree to share knowledge on the research and use of ultra-deep geothermal energy in the process industry and in the heating of the build environment and greenhouses. More importantly, the goal is to set-up multiple UDG projects in a foreseeable timeframe (Green Deal UDG, 2017).

One of the formations which is expected to have a high geothermal potential are the Lower Carboniferous Dinantian platform carbonates, known as the Zeeland formation (van Hulten & Poty, 2008). The relative small number of wells (24) (EBN , 2019) in the Netherlands that penetrate this formation are mostly

clustered along the margins of the NW European Carboniferous Basin (NWECB) in the South of the country. Apart from the UHM-02 well and LTG-01 well which are located in the North of the country, and the WSK-01 well which is located in the middle of the country (Figure 1). Due to the limited amount of available seismic and well data, the Zeeland Fm. is currently under-explored and consequently the geothermal potential is not completely proven (Reijmer, ten Veen, Jaarsma, & Boots, 2017).

1.2 Study objective

The objective of this study is to verify the potential of the Dinantian carbonates as a geothermal reservoir on a local scale. To do this, the Californië wells in Limburg (NL) have been used as a case study. These wells are currently the only geothermal wells in the Netherlands that are penetrating the Dinantian carbonates. Therefore, the goal is to create a dynamic reservoir model that confirms the production data of the wells (pressure/flow/temperature) and can explore the geothermal potential of the reservoir in space and time. This study will *not* make a statement about possible seismicity related to the wells.

1.3 Case study

The Californië wells are located in the greenhouse area 'Californië', near the village of Grubbenvorst in Limburg (NL). The wells form 2 separate doublets. The first doublet has been drilled in 2012 and is owned by Californië Wijnen Grubbenvorst (CWG). It consists of one producer (CAL-GT-01S) and one injector (CAL-GT-03). Initially, the doublet included a third well (CAL-GT-02), but it collapsed due to poor hole conditions. The second doublet has been drilled in 2015 and is owned by Californië Lipzig Gielen (CLG). It consists of one producer (CAL-GT-04) and one injector (CAL-GT-05). Well CAL-GT-01 and CAL-GT-05 have an open hole completion. Well CAL-GT-03 has a slotted liner and open hole section, however the open hole section is plugged and does not show flow on the production logging tool (PLT). Well CAL-GT-04 is perforated.

The wells are drilled in the NE-edge of the Roer Valley Graben, close to the Tegelen fault. The Tegelen fault is a NW-SE striking normal fault with a large offset; approximately 100-200m in the lower Carboniferous (based on the static model in this paper). The wellbore trajectory of wells CAL-GT-01S, CAL-GT-03 and CAL-GT-04 intersect the Tegelen fault zone. Hence, the Tegelen fault zone forms an important structural element in the static reservoir model. Well CAL-GT-02 and CAL-GT-05 are drilled in opposite direction.

The depositional system of the Dinantian carbonate sequence in the Californië area remains unclear. The absence of deep-water facies in the cuttings of CAL-GT-01S (Poty, 2014), suggests that the carbonate formation was part of a large carbonate ramp system stretching from the Netherlands towards Belgium, forming a carbonate platform in the Californië area. However, it cannot be excluded that a structural high existed at the time of deposition. Both depositional environments explain the thickness differences of the Zeeland Fm. in the different wells.

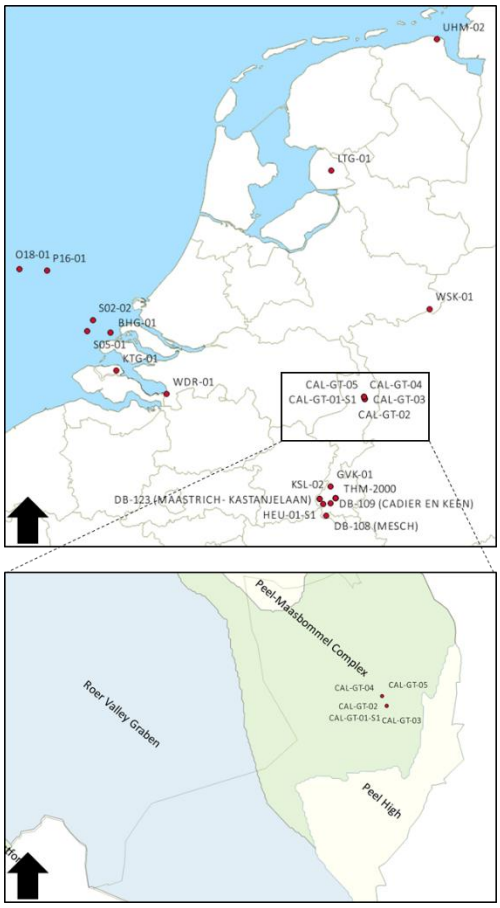

Figure 1. Location of the Californië wells in Limburg (dots = wells that penetrate Dinantian carbonates) (background: structural elements in the Netherlands, based on (Kombrink, et al., 2012))

2. INPUT DATA

The available input data for the static and dynamic reservoir model is limited. Primarily, the static model is based on two 2D seismic lines shot in 2010. The wellbore trajectory of all four wells is deviated and not positioned along the seismic lines. Consequently, a well-to-seismic tie is not available. Next to this, CAL-GT-01S is the only well with an extensive logging suite. It includes a gamma ray log (GR), sonic log, dipole shear sonic imager log (DSI), resistivity log, caliper, nuclear magnetic resonance log (CMR), spontaneous potential log (SP) and a formation micro imager log (FMI). All logs cover different parts of the wellbore of CAL-GT-01S. The only available logs in the other wells are the gamma ray log (GR) and caliper. All wells have a litho-log based on the cuttings.

The Tegelen fault zone forms the main structural element in the static model. To obtain an insight in the fault zone architecture of this fault, a fieldwork has been executed in a quarry (Germany), named Hastenrath. The Hastenrath quarry is situated near Aachen in the Stolberg area. From a structural point of view, the Hastenrath quarry is positioned along the Sandgewand fault, which is also a large offset (≈300-

500m at base Carboniferous) normal fault and part of the SE-edge of the Roer Valley Graben (Becker, et al., 2014).

The available well test data includes a production well test of CAL-GT-01S, injection well test of CAL-GT-02, multiple PLT's in CAL-G-03 and CAL-GT-05, production well test in CAL-GT-04, production and injection well test in CAL-GT-05 and an interference test between both doublets. Most of the well test data is low quality (few data points) and often the pressure and flow measurements are not sufficient (very short build-up/fall-off period) for Pressure Transient Analysis (PTA).

The available production data of both doublets forms the main input for the dynamic modelling. For both doublets it includes injection pressure, injection temperature, flow rate (at surface) and production temperature. The available production data of the CWG doublet also includes the ESP pressure and frequency.

3. FIELDWORK

The carbonate formations observed in the Californië wells and the Hastenrath quarry have been deposited in a similar time frame under similar conditions. This conclusion is based on the corresponding structural setting, depositional environment of both locations (carbonate platform) (Poty, 2014) (Becker, et al., 2014) and fracture orientation (NW-SE) observed at the both locations (FMI results of CAL-GT-01S) (Becker, et al., 2014). However, the burial history of both locations differs, because the Hastenrath quarry is located in the Variscan fold-and-thrust belt of the Rhenohercynian (Becker, et al., 2014). This could result in more folding related features in the Hastenrath quarry, compared to the Californië area.

3.1 Methodology

The fault zone architecture of the Tegelen fault forms an essential element in the static property model, because it influences the permeability distribution in the reservoir. Figure 2 displays a generic fault zone architectural model. It consists of a fault core enveloped by a damage zone, bounded by the background fracture network. The fault core is an area of highly localized strain and accommodates a large part of the displacement of the fault (Choi, Edwards, Ko, & Kim, 2016). The adjacent damage zone is characterized by low strain and less intense deformation. It exhibits small scale structural discontinuities, such as fractures, veins and deformation bands. The criteria to define the boundary between the damage zone and the background fracture network remain debated, however the fracture frequency is a commonly used parameter (Choi, Edwards, Ko, & Kim, 2016).

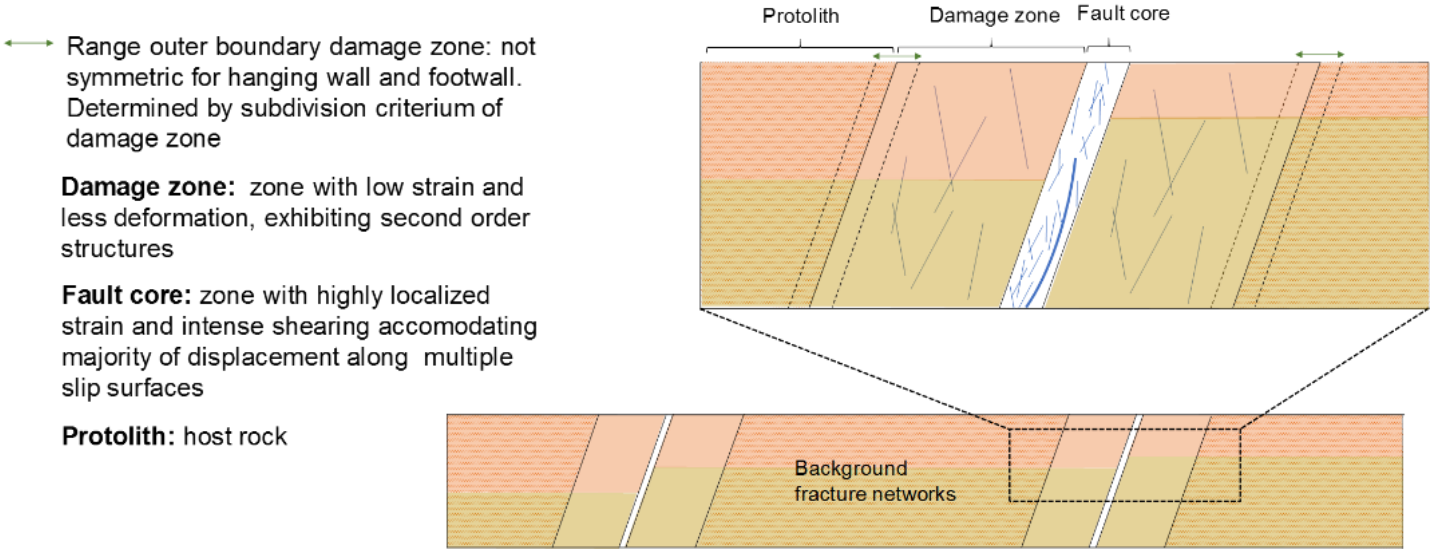

Figure 2. Fault zone architecture (Image based on description in literature (Choi, Edwards, Ko, & Kim, 2016) (Michie, et al., 2014) (Berg & Skar, 2005))

The permeability in the damage zone is defined by the presence of macro-scale fracture networks and deformation/compaction features, which both decrease in frequency at increasing distance from the fault core (Faulkner, et al., 2010). A measure for fracture frequency is the fracture density, which can be defined according to multiple definitions. The permeability in the damage zone is a function of the observed fracture network density (Mitchell & Faulkner, 2012).

The main goal of the fieldwork in the Hastenrath quarry is to obtain a value for the maximum damage zone width of the Sandgewand fault, which is thought to be comparable to the Tegelen fault. The width of the damage zone has been established by evaluating the fracture network density with a scanline analysis on multiple outcrop surfaces in the quarry. The scanline analysis is performed in Digifract (TU Delft software), a software in which the fractures, visible in the georeferenced photographs, can be manually digitized and analysed. The fracture density along each scanline corresponds to the amount of fracture intersections divided by the length of the scanline. By selecting multiple outcrop surfaces at varying distance from the Sandgewand fault core, the spatial development of the fracture density is captured. The main selection criteria

for the outcrop surfaces is the requirement to capture the NW-SE striking fractures, which correspond to the fracture orientation visible in the FMI of CAL-GT-01S.

3.2 Results

Seven different outcrop surfaces have been analysed in the Hastenrath quarry. Figure 3 is a top view of the quarry showing the quarry contours (blue), Sandgewand fault (red) and outcrop surfaces (black dots). Figure 4 shows an image of an outcrop surface and the digitalisation of the fractures and bedding planes. A decrease of the fracture density can be related to the presence of a bedding plane, which implies that the bedding planes may form a boundary for fracture propagation.

Each of the analysed outcrop surfaces is characterized by an average fracture density (see table in figure 3). All outcrop surfaces show an average fracture density within a similar range (1-2,2 fractures/m). This might suggest that all measured outcrop surfaces are located in the background fracture network and not within the damage zone of the Sandgewand fault. Hence the distance between the core of the Sandgewand fault and outcrop surface HAS2 (outcrop located closest to the fault core) is an indication for the maximum damage zone width, based on the assumption that the Sandgewand fault is the only major fault in the quarry with a significant damage zone. The distance equals 80 meters. Due to mining activities, outcrop surfaces closer to the fault core could not be analysed. In the study of Becker (2014) scanlines closer to the fault core have been analysed. The results show a 50% decrease of the average fracture density within approximately 50m of the fault core, which suggests that the boundary of the damage zone is within a similar range. This is in accordance with the results of this study. Observations in the quarry prove that multiple smaller offset faults parallel to the Sandgewand fault are present. The possibility exists that these smaller offset faults are also enveloped by a thin damage zone that could function as a pathway for flow in the tight carbonates. This hypothesis is processed in the permeability scenarios in the static property model.

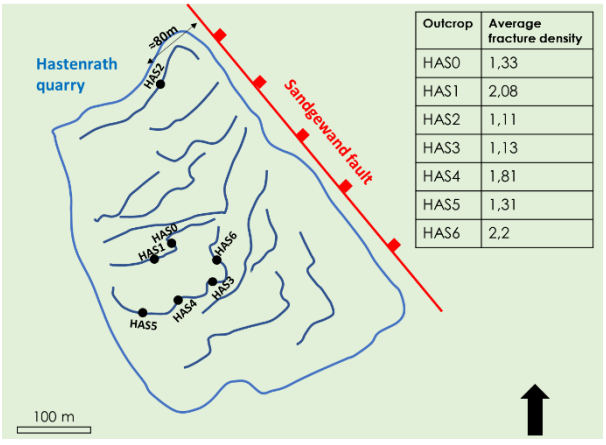

Outcrop	Average fracture density
HAS0	1,33
HAS1	2,08
HAS2	1,11
HAS3	1,13
HAS4	1,81
HAS5	1,31
HAS6	2,2

Figure 3. Top view of the Hastenrath quarry showing the average fracture density measured in each outcrop surface

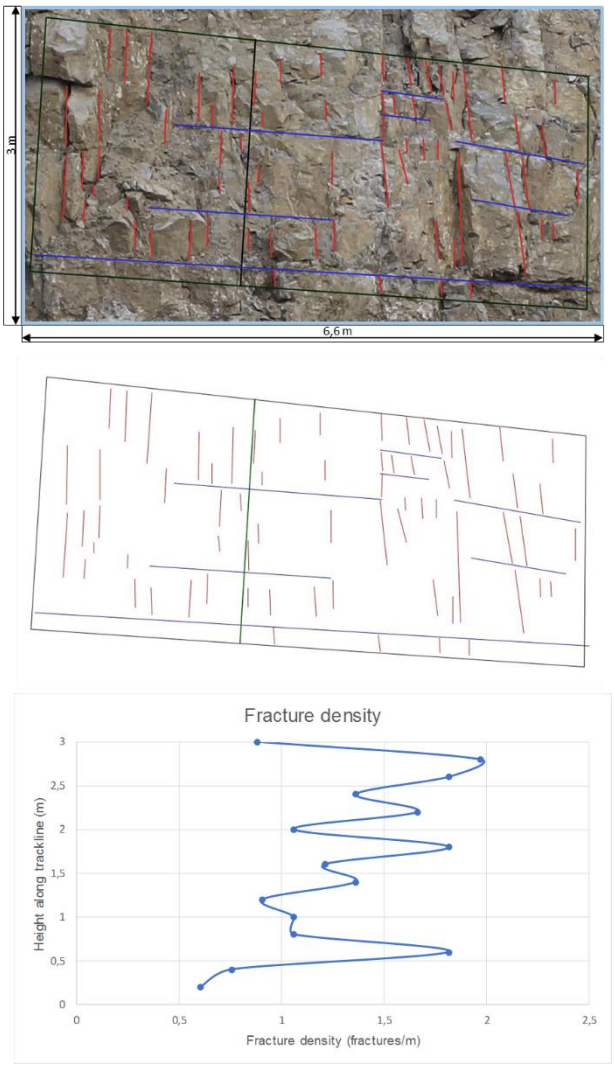

Figure 4. Scanline analysis HAS5 (red=fractures, blue = bedding planes, green = trackline, yellow = fracture density)

4. STATIC MODEL

4.1 Methodology

The reservoir geometry and spatial development of each formation between the seismic lines and wells can only be approximated by extrapolation of the available data. Due to the limited amount of available data, the following approach has been adapted for each *step* in the static model development:

1. The *seismic interpretation* is based on high amplitude seismic reflectors.
2. The *well top interpretation* is based on the GR log and Litho-log (derived from cuttings).
3. The *time-depth conversion* is established using a layer-cake model with a fixed interval velocity for each horizon. For the velocity estimation, an alternative method has been applied, as a local subsurface seismic velocity model (based on for instance VSP/check shot) is unavailable. The interval velocity of the top three horizons (Base North Sea Group (NSG), Base Chalk and Base Permian Unconformity (PU)) has been based on pseudo-velocities,

deducted from seismic picks and formation tops in the wells. The interval velocity of the bottom two horizons (Base Limburg and Base Zeeland) has been derived from the sonic velocity of offset wells.

4. The *structural model* is constructed with the following assumptions in mind:
    a. All structural elements follow the general NW-SE striking trend of the Roer Valley Graben
    b. The structural high/platform geometry is present in all formations and has a constant thickness
    c. The Tegelen fault is a normal fault.

    Two additional horizons have been added in the structural model (Base Bosscheveld and Base Condroz) using a constant thickness based on well data. All horizons have been edited manually using additional grid point sets for each surface.

For the *property model*, it is assumed that the reservoir consists of the Zeeland formation (Dinantian), Bosscheveld formation (Devonian) and Condroz group (Devonian). The Limburg formation (Silesian) and Pont d'Arcole (lower Dinantian) are assumed to function as a seal. This subdivision is based on the completion of the wells, the loss zones reported during drilling, the PLT in CAL-GT-03 and CAL-GT-05, the FMI in CAL-GT-01S and the caliper logs.

A rough estimation of the average porosity for each formation has been calculated with the Wyllie equation using the sonic log and DSI log of well CAL-GT-01S. For the Zeeland Fm., Bosscheveld Fm. and Condroz grp. a dolomite matrix slowness of 144 µs/m and a fluid slowness of 620 µs/m has been applied (based on the Litho-log), in combination with a clean sandstone GR of 20 API and a 100% shale GR of 120 API (based on the GR reading in the Pont d'Arcole). The Net-to-Gross ratio (N/G), water saturation (Sw) and shale volume (Vshale) values (0 or 1) are based on the distinction between reservoir and non-reservoir formation.

The permeability distribution in the reservoir intervals is based on the results of the fieldwork executed in the Hastenrath quarry. It is assumed that all reservoir intervals display a similar uniform distribution of permeability features. More importantly, it is assumed that the reservoir is a single porosity system, implying that the primary matrix porosity and permeability are negligible. This assumption is based on the derived porosity value from the sonic log, which is very low. Consequently, it is assumed that the permeability in the system is fault, fracture and karst related. The distribution of faults, fractures and karst in the reservoir is unknown. Therefore, multiple permeability scenarios have been created in the static property model, in which the distribution of these structural features have been varied. The goal is to create an optimum permeability distribution for which the dynamic model results match the production data. The well test analysis of CAL-GT-05 provides a reference for the permeability value of the background fracture network, because CAL-GT-05 does not intersect high permeability features, such as large fault zones or karst (proven in PLT/well logs). This is validated by the resulting permeability value, which is very low. The permeability in the damage zone is defined based on an exponential declining function derived from literature.

At last, the static model is upscaled to a resolution of 100x100m grid cells. As a result, the damage zone of the Tegelen fault is upscaled to a width of 100m, which leads to a slight overestimation of the permeability in the fault zone in the static model.

4.2 Results

4.2.1 Seismic interpretation & Well top identification

The GR and Litho-log (based on cuttings) are used to identify 6 different formation tops in each well; base NSG, base Chalk, base PU, base Limburg, base Zeeland and base Bosscheveld. The stratigraphic column is characterized by two hiatuses; a disconformity at the base Chalk and an angular unconformity at the base of the Zechstein (base PU). The base Zeeland is characterized by the top of the Pont d'Arcole, a thin shale layer, which is part of the Bosscheveld formation (Devonian) in this study. The base Bosscheveld is marked by the presence of the first clastic in the Litho-log. The base Condroz cannot be identified in the wireline logs.

The wells are projected along a 135 degrees azimuth angle onto the seismic line, to provide an indication for the corresponding reflector along the vertical section of the well. Figure 5 shows a simplified interpretation of the 09-02 seismic line. The base Bosscheveld and base Condroz cannot be interpreted in the seismic line, due to low seismic resolution.

The seismic line shows the onlap of the Namurian shales (Limburg Fm.) onto the Dinantian carbonates (Zeeland Fm.). The bright reflectors within the Zeeland Fm. may be caused by the karst features, which are encountered in the well log data. The high amplitude reflectors in the Limburg Fm. may be related to coal seams, dating from the Westphalian.

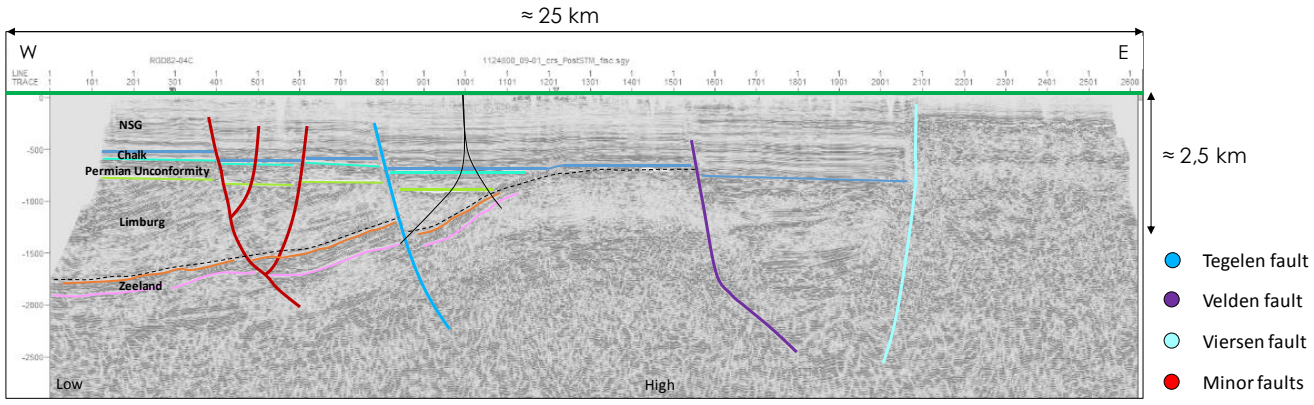

Figure 5. Simplified seismic interpretation of the 09-02 line showing a conceptual model of the subsurface (black lines indicate the well trajectories)

The Tegelen fault is the only fault visible on both seismic lines and therefore this is the only fault incorporated in the static model. It cannot be assumed that all the other faults are parallel to the Tegelen fault, because multiple fault orientation trends have been observed at different locations in the Netherlands in the Carboniferous (ter Borgh, 2017).

The time-to-depth conversion is accurate for the top three horizons, implying that the modelled surfaces (in depth) cross the well trajectories next to the previously defined well tops. For the Limburg and Zeeland formation, the derived fixed interval velocity is too high, which results in modelled surfaces which are too deep. To ensure that the modelled surfaces are within the same depth range as the well tops, a 200-meter depth correction has been applied.

4.2.2 Structural model

The surfaces (depth converted) and Tegelen fault are edited using grid point sets. The grid point sets are applied to modify the surfaces, based on the depth values observed on the seismic line and the criteria named in the methodology. Next, the average base Bosscheveld thickness is derived from the well data (average thickness of 243m), whereas the base Condroz is placed based on trial and error (thickness of 900m), taking into account that the surface cannot cross the well trajectories.

4.2.3 Property model

Table 1 provides the applied values for N/G, Sw and Vshale for the different formations. The resulting Wyllie equation porosity for the Zeeland formation equals 6%, which is relatively high for a tight carbonate formation, considering an average porosity of <2% for the Dinantian interval in other wells in the country (EBN , 2019). According to the authors of EBN (2019) the application of a limestone matrix slowness (160 µs/m) results in a porosity estimation which shows better correspondence with the total porosity derived from the CMR. The resulting porosity estimation of the Zeeland Fm. in CAL-GT-01S is also elevated compared to the other wells, which is in accordance with our study. The Bosscheveld Fm. is characterized by a porosity value of 4% and the Condroz group by a porosity value of 1%, which shows that these reservoir formations are also tight.

Zone	N/g	Sw	Vshale
Limburg	0	0	1
Zeeland	1	1	0
Pont d'Arcole	0	0	1
Bosscheveld	1	1	0
Condroz group	1	1	0

Table 1. N/G, Sw, and Vshale for each formation in the static property model

The focus of the static property model lies on the permeability distribution. Each scenario corresponds to a permeability distribution, which is characterized by a specific configuration of "permeability building blocks". Three different building blocks exist: the fault and damage zone, the background fracture network and the high permeable layers. Figure 6 shows the difference building blocks in a conceptual cross section of the model. Based on the matching criteria in the dynamic model, a specific combination of building blocks will be defined, named 'best-case scenario'.

The first building block corresponds to the Tegelen fault zone. The permeability (K) (equation 2) in the damage zone depends on the fracture density (F) function (equation 1) (derived from (Mitchell & Faulkner, 2012)). Parameter B and C are defined using the permeability value from the well test results as a reference for the value at the edge of the damage zone, keeping in mind that the Tegelen fault zone forms a good conduit for flow.

$$F = e^{-\frac{x}{A}} \quad [1]$$

$$K = F^B * C \quad [2]$$

X = distance to fault
A = width of the damage zone (A=100m)
B = coefficient determined by trial and error (B=5)

C = permeability if the fracture density equals 1 (corresponds to permeability at the fault core in this model) (C=500 mD)

The background fracture network and high permeable layers (second and third permeability building block) are characterized by a homogeneous distribution, equal to a single value for permeability. Each high permeable layer is characterized by a unique permeability value, which is defined based on the matching criteria in the dynamic model.

A permeability anisotropy is applied throughout the entire model. The NW-SE oriented Tegelen fault and the NW-SE oriented fractures, visible in the FMI of CAL-GT-01S, define the permeability component parallel to the Tegelen fault (Kj) to be the main conduit for flow. For the damage zone, this component is equal to the permeability calculated in equation 2. For the background fracture network, the geometric average of all three values (equation 4) must be within the same range as the result of the well test analysis of CAL-GT-05.

$$K_j = K \quad [3]$$

$$K_i = K_k = \frac{K_j}{10} \quad [4]$$

5. DYNAMIC MODEL

5.1 Methodology

The aim of the dynamic model is to obtain a match between the simulated pressure and flow rate in the model and the recorded pressure and flow rate in the production data (history match). The permeability distribution in the static property model forms the main variable to attain the history match. The pressure and flow rate values in the production data function both as a control mode in the model and as a reference value in the history match. For well CAL-GT-01S, CAL-GT-04 and CAL-GT-05 the control mode in the dynamic model is the flow rate, which means that the focus lies on the pressure match with the production data. For well CAL-GT-03, this is the opposite.

The surface pressures are converted to a bottom hole pressure (BHP) by approximating the pressure drop in each wellbore. Next, it is assumed that the produced water volume equals the injected water volume, resulting in similar flow rates as reference value in the model. The production data has been subdivided into spring/summer and autumn/winter seasons. This subdivision is also applied in the timeline of the dynamic model.

The thermal modelling is based on the following parameters; the injection temperature (retrieved from the production data), the temperature gradient (assumed to be 33 °C/km with 11 °C surface temperature), the specific heat of rock and water and a value for the thermal conductivity of the reservoir rock. This means that the main thermal recharge mechanism is the rock conductivity and that only forced fluid convection is included. Free fluid convection from adjacent layers and along the Tegelen fault zone is not considered in this study.

The following *criteria* must be met, when defining the best-case permeability scenario:

1. The simulated flow rate and production temperature must match the production data
2. The simulated BHP must match the calculated reference BHP (derived from the surface pressure recorded in the production data)
3. CAL-GT-03 cannot inject below base Zeeland (based on the PLT, which shows no flow below base Zeeland, due to a natural obstruction)
4. CAL-GT-05 mainly injects in the Condroz grp. and only a small volume of water in the Zeeland Fm. (based on the PLT)
5. The value of each permeability block must be maintained within a realistic range

5.2 Results

5.2.1 Best-case scenario: permeability configuration

Figure 7 depicts the different permeability features and corresponding dimensions in the best-case scenario, which has been defined based on the matching criteria. Table 2 provides the associated permeability values applied in each permeability building block. The fault transmissibility is equal to 1, implying a fully transmissible fault.

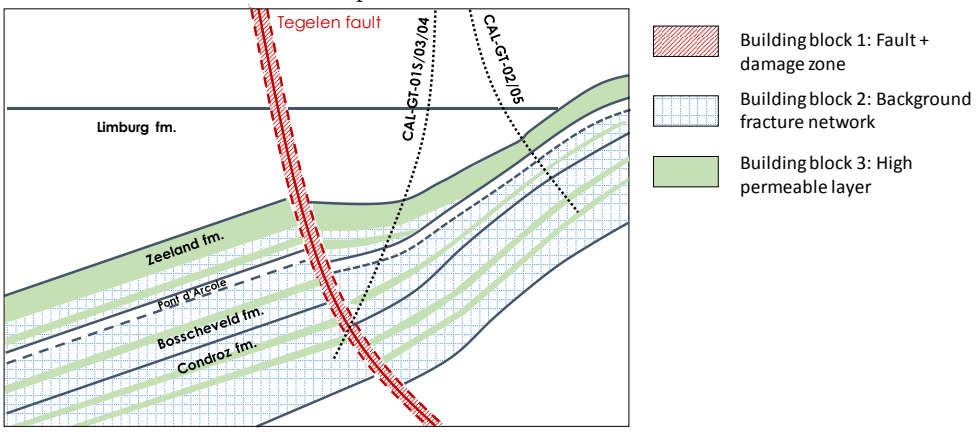

Figure 6. Permeability building blocks implemented in the static property model

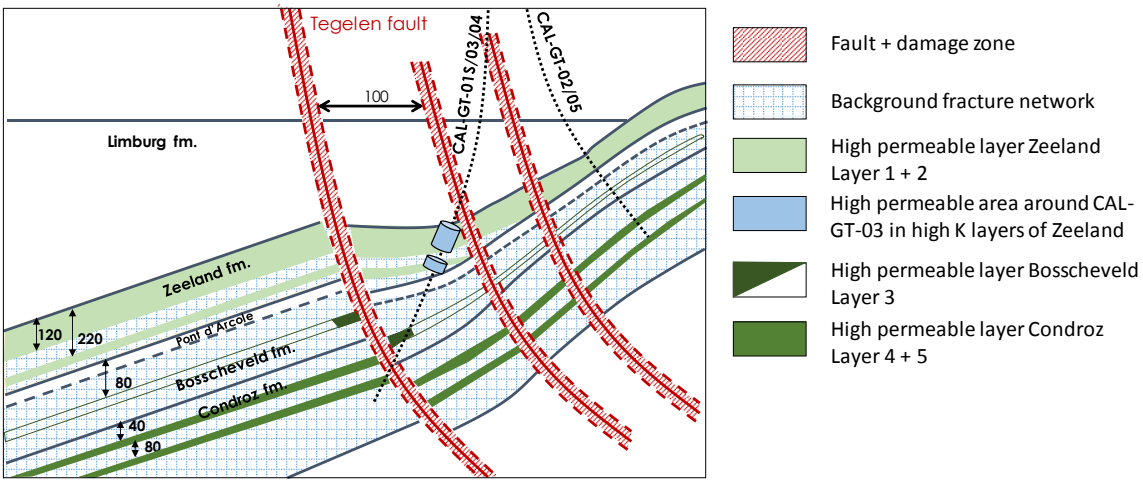

Figure 7. Conceptual model of the permeability configuration in the best-case scenario

Component	Value Kj [mD]	Geometric mean [mD]
High K zone around CAL-GT-03 in high K layers of the Zeeland Fm.	2000	431
High K layer 1 & 2 [Zeeland Fm.]	30	6,5
High K layer 3 [Bosscheveld Fm.]	250	54
High K layer 4 & 5 [Condroz group]	250	54
Background fracture networks	15	3,2
Tegelen fault core	500	108
Faults parallel to Tegelen fault	50	11

Table 2. Permeability value of the different permeability building blocks in the best-case scenario

From figure 7 and table 2 becomes clear that the best-case scenario includes a Tegelen fault zone, characterized by a Kj value of 500 mD at the fault core, which decreases exponentially over 100 meters away from the fault core. Next, the model includes parallel faults to the Tegelen fault, characterized by a Kj value of 50 mD. Each fault zone is 100-meter wide (one grid cell), which means a damage zone of 50 meter. Five different high permeable layers are included in the model. The layer in the Bosscheveld formation is only based on the intersection of the Tegelen fault with well CAL-GT-01S. It is not recognized in the PLT of other wells, and therefore it is not continuous. The high permeable layers in the Zeeland Fm. require a cylinder of extremely high permeability around the wellbore of CAL-GT-03 to attain the injected volume recorded in the production data. The initial well logs of CAL-GT-03 do not show any large karst features or fracture corridors. Consequently, the large injectivity of well CAL-GT-03 might be related to an enhancement of reservoir permeability over time. Between the high permeable layers and the fault zones, the model is filled with a background fracture network, characterized by a Kj of 15 mD, which is equal to a geometric average of 3,2 mD. This is within the same order of magnitude as the well test results of CAL-GT-05 for permeability.

5.2.2 Best-case scenario: BHP and flow rate results

Figure 8 depicts the BHP plot and figure 9 the flow rate plot for the best-case scenario.

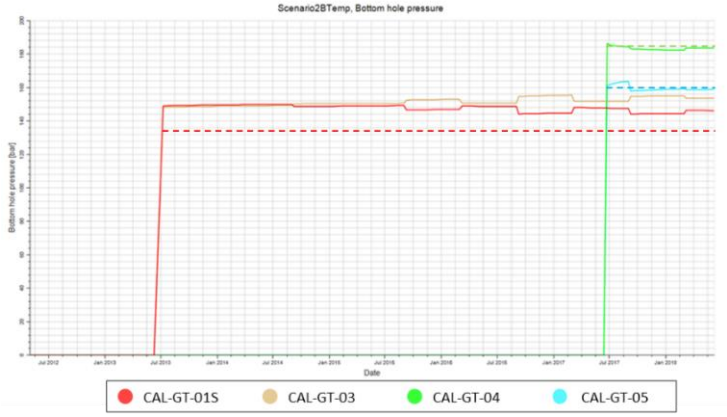

Figure 8. BHP plot for the best-case scenario (solid line = simulated value, dotted line = reference value)

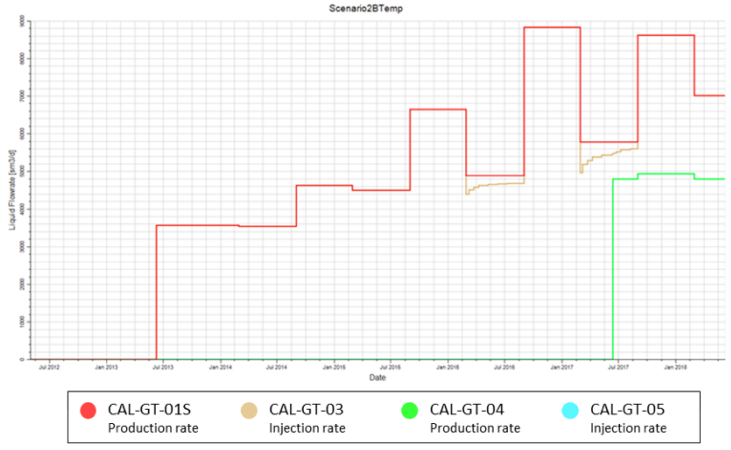

Figure 9. Flow rate plot for the best-case scenario (solid line = simulated value, dotted line = reference value)

The BHP match between the model results (solid line) and production data (dotted line) is accurate for CAL-GT-04 and CAL-GT-05. In contrary, the simulated BHP of CAL-GT-01S does not correspond to the reference value. The main reason for this is the increased productivity of well CAL-GT-01S over time. From both the BHP and flow rate plot it becomes clear that the pressure in well CAL-GT-01S and CAL-GT-03 remains constant over time, whereas the flow rate significantly increases. This is most likely related to a change in the reservoir system, accompanied by an enhancement of reservoir properties over time. These time dependencies cannot be captured in the current model.

Next to this, CAL-GT-01S and CAL-GT-03 are located next to each other, which results in interference in the model. This becomes clear from the streamline plots (Reith, 2018), which show that the injected water from CAL-GT-03 is mainly directed to CAL-GT-01S. Consequently, the modelled homogeneous high permeable cylinder around the wellbore of CAL-GT-03 proves to have a negative influence on the BHP match of CAL-GT-01S with the production data. From this can be concluded, that the reservoir must be extremely heterogeneous.

The tracers in the model show that CAL-GT-01S produces mainly from the Zeeland Fm. and CAL-GT-04 produces mainly from the Condroz group (Reith, 2018). There are no PLT's available to check this result. Next to this, the interference between the CLG and CWG doublet in the model has been tested. The results indicate that CAL-GT-01S produces more water from the Condroz group without the presence of CAL-GT-04, resulting in a temperature difference of 1 °C at the end of the simulated timeframe. This corresponds to the results of the interference test, which show that CAL-GT-04 responds to water injection in CAL-GT-03 and CAL-GT-05. CAL-GT-01S is not included in the interference test, but since it is located between CAL-GT-04 and CAL-GT-03, the interference between CAL-GT-04 and CAL-GT-01S is very likely.

3.3.3 Best-case scenario: Temperature results

Figure 10 depicts the simulated production temperature (solid line) and the reference value (dotted line) from the production data.

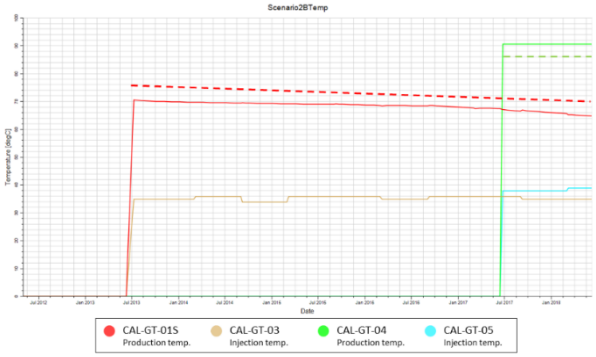

Figure 10. Temperature profile for the best-case scenario (solid line = simulated value, dotted line = reference value)

It becomes clear that the simulated temperature profile for CAL-GT-01S and CAL-GT-04 does not show a match with the reference values for the best-case permeability scenario. Regarding the simulation results, it appears that CAL-GT-01S should be producing from deeper layers, whereas the main production interval of CAL-GT-04 must shift upwards. However, the simulated production temperature profile does capture the decreasing production temperature of CAL-GT-01S, which is partly due to the interference with CAL-GT-04 (1 °C) and mainly due to the thermal rock conductivity of the reservoir (3 °C).

Two sensitivity studies have been conducted to define the source of mismatch between the model and the data. The first sensitivity evaluates the permeability configuration in the model; by changing the completion of the wells, the production intervals are altered. Consequently, the simulated BHP and flow rate match are also affected. The results show that a correct temperature profile for CAL-GT-01S can be obtained by stimulating the production from the base of the Condroz group, whereas the contrary is necessary for well CAL-GT-04. This result verifies the heterogeneity of the reservoir and identifies the potential of the Condroz group.

The second sensitivity builds on the original permeability configuration defined in the best-case scenario but alters the temperature gradient. The results show that CAL-GT-01S requires a temperature gradient of 36 °C/km to produce at the correct temperature, whereas CAL-GT-04 requires a temperature gradient of 31 °C/km. To identify the accuracy of these thermal gradients, offset wells in the region can be used as a reference. The figure below shows the location and temperature gradients in well AST-01, NVG-01, KDK-01 and AST-GT-02 (EBN, 2018). All wells have a thermal gradient in the range 30 °C/km to 35 °C/km, apart from AST-GT-02, which only has 2 temperature measurements. From this can be deducted, that the calculated thermal gradients of CAL-GT-01S and CAL-GT-04 are not out of range. However, the large difference (5 °C/km) in thermal gradient of CAL-GT-01S and CAL-GT-04 is unlikely to exist simultaneously in the reservoir from which the wells are producing. This would require structural compartmentalization and/or significant variation in rock properties and reservoir properties, which are both questionable, because the wells are less than 1,5 km apart.

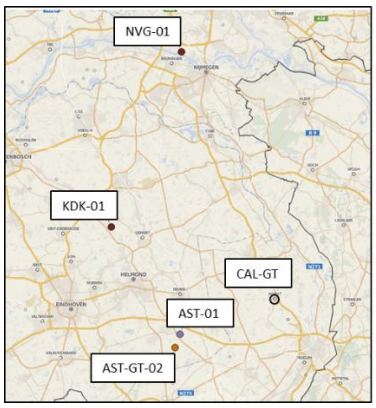

Well	Temperature gradient (°C/km)
NVG-01	35,0
KDK-01	31,9
AST-01	29,5
AST-GT-02	25,3

Figure 11. Temperature measurements and resulting thermal gradient of regional offset wells (EBN, 2018)

6. DISCUSSION

The best-case permeability scenario in this study confirms the heterogeneity and complexity of the subsurface in the Californië area. The created static and dynamic model consider all the available data; however, a large framework of assumptions has been necessary to approximate the missing geological parameters. Consequently, the permeability configuration applied in the best-case scenario is not unique for the Californië reservoir; multiple variations can be assessed if additional data becomes available.

The most important limitations of the best-case scenario are the following;

1. The model does not incorporate the upwelling of (warmer) water from deeper layers and along faults (free convection)

2. The model does not incorporate a general ground water flow or energy flux

3. The model is single-porosity and assumes all flow mechanisms (karst/fractures/faults) to have a uniform distribution in space, characterized by a constant value for permeability. This is considered unlikely.

4. The simulations in the dynamic model are based on a single static model; the changing reservoir properties and characteristics over time are not considered.

The limitations of the implemented modelling software have a minimum effect on the results in this study, because the reservoir is part of the low-enthalpy regime (<100 °C), resulting in single phase fluid flow. Next to this, the applied workflow in this study is oversimplified. For future modelling of fractured carbonate reservoirs, the workflow must be extended by incorporating geo-mechanical studies to define the development of fracture aperture as a function of state of stress in a specific area and as a function of time. The thermal effect on the fracture aperture and propagation must also be taken into account, to be able to define the heat transfer in the reservoir more accurately. Implementing coupled modelling of flow and mechanical properties, as a function of pressure and temperature is therefore necessary to estimate the thermal breakthrough moment in the reservoir, which defines the long-term development of the geothermal field.

7. CONCLUSION

This study presents a dynamic reservoir model of a heterogeneous and tight Dinantian carbonate reservoir, that not only proves the geothermal potential of the Dinantian carbonates, but also the geothermal potential of the Devonian Bosscheveld formation and Condroz group.

In this study a best-case permeability scenario has been created, that provides an optimum match between the dynamic modelling results (pressure/flow) and the production profile of the Californië wells. The simulated temperature profile does not show an acceptable history match; however, it does capture the temperature decrease, which is also visible in the production data. The fact that all three dynamic parameters (pressure/flow/temperature) cannot be matched within a single permeability scenario, is the proof that the reservoir is extremely heterogeneous and complex.

Due to the lack of data, the depositional setting of the reservoir, the reservoir geometry and the reservoir properties are largely unknown. Consequently, an extensive framework of assumptions has been constructed to approximate all the geological parameters. This framework forms a large uncertainty in the project, together with the main modelling limitations.

To optimize and validate the static and dynamic model, additional data acquisition is highly recommended. If this is acquired and the workflow is optimized, the model will gain more predictive power for the life-cycle of the geothermal reservoir and future field development.

REFERENCES

Becker, S., Nguyen, H., Nollet, S., Fernandez-Steeger, T., Laux, D., & Hilgers, C. (2014). Methods to analyse fracture orientation patterns in a Lower Carboniferous carbonate reservoir analogue in the Voreifel, Germany. *German Journal of Geology*, 319-330.

Berg, S., & Skar, T. (2005). Controls on damage zone asymmetry of a normal fault zone: outcrop analyses of a segment of the Moab fault, SE Utah. *Elsevier* , 1803-1822.

Choi, J., Edwards, P., Ko, K., & Kim, Y. (2016). Definition and classification of fault damage zones: A review and a new methodological approach. *Elsevier*, 70-87.

EBN . (2019). *SCAN Dinantian Report (in preparation).*

EBN. (2018). Pressure Database in Spotfire.

Faulkner, D., Jackson, C., Lunn, R., Schlische, R., Shipton, Z., Wibberley, C., & Withjack, M. (2010). A review of recent developments concerning the structure, mechanics and fluid flow properties of fault zones. *Journal of Structural Geology*, 1557-1575.

Green Deal UDG. (2017). *Green Deal Ultra-diepe geothermie (UDG).* Retrieved from Platform Geothermie: http://www.geothermie.nl/images/bestanden/Green_Deal_UDG_tekenversie.pdf

Kombrink, H., Doornenbal, J., Duin, E., Den Dulk, M., Gessel, S., ten Veen, J., & Witmans, N. (2012). New insights into the geological structure of the Netherlands; results of a detailed mapping project. *Netherlands Journal of Geosciences*, 419-446.

Michie, E., Haines, T., Healy, D., Neilson, J., Timms, N., & Wibberley, C. (2014). Influence of carbonate facies on fault zone architecture. *Elsevier*, 82-99.

Ministry of Economic Affairs and Climate Policy. (2013). *Energy Agreement for Sustainable Growth.*

Ministry of Economic Affairs and Climate Policy. (2017). *Energy Agenda.* Retrieved from Government of the Netherlands: https://www.government.nl/documents/reports/2017/03/01/energy-agenda-towards-a-low-carbon-energy-supply

Mitchell, T., & Faulkner, D. (2012). Towards quantifying the matrix permeability of fault damage zones in low porosity rocks. *Earth and planetary science letters*, 24-31.

Poty, E. (2014). *Cuttings report CAL-GT-01S.*

Reijmer, J., ten Veen, J., Jaarsma, B., & Boots, R. (2017). Seismic stratigraphy of Dinantian carbonates in the southern Netherlands and northern Belgium. *Netherlands Journal of Geoscience*.

Reith, D. (2018). *Dynamic simulation of a geothermal reservoir (Msc Thesis).* Retrieved from TU Delft Repository: https://repository.tudelft.nl/islandora/object/uuid:e38ecf05-dfc1-4bcc-b995-875e178609dc?collection=education

ter Borgh, M. (2017). *Internal reporting EBN B.V.*

van Hulten, F., & Poty, E. (2008). Geological factors controlling Early Carboniferous carbonate platform development in the Netherlands. *Geological Journal 43*, 175-196.